STUDY ON HIGH ORDER MODES DRIVEN LONGITUDINAL COUPLED-BUNCH INSTABILITIES IN HALF STORAGE RING*

W. Li, T. He†, X. Liu, Z. Bai
National Synchrotron Radiation Lab., University of Science and Technology of China, Hefei, China

Abstract

Longitudinal higher-order modes (HOMs) trapped in vacuum components such as gate valves are a potential source of coupled-bunch instabilities in the HALF storage ring. Using macroparticle tracking simulations, we study these instabilities under bunch lengthening provided by a passive third-harmonic cavity. Two distinct instability types are identified: a centroid-oscillation mode and an energy-spread-growth mode. The former can be suppressed by a longitudinal feedback system, while the latter cannot. Quantitative thresholds as a function of HOM frequency with different bunch distributions are obtained to guide the impedance optimization of HALF vacuum components.

INTRODUCTION

The Hefei Advanced Light Facility (HALF) is a fourth-generation diffraction-limited storage ring currently under construction, with a design target beam current of 350 mA [1]. Designed to deliver ultra-low emittance and high brilliance, HALF operates with a low momentum compaction factor, making it inherently sensitive to collective effects that can limit its performance [2].

Higher-order modes (HOMs) are electromagnetic resonances that can be excited by a particle beam as it interacts with surrounding structures, potentially driving coupled-bunch instabilities and leading to beam loss. In the HALF storage ring, both the main RF cavities (MC) and the passive third-harmonic cavity (HC) are designed as superconducting cavities, whose intrinsic HOMs are expected to be heavily damped through dedicated absorbers. Consequently, the primary concern for HOM-driven instabilities shifts to other vacuum components, most notably the gate valves. A similar situation was encountered at the SIRIUS light source: unanticipated longitudinal coupled-bunch instabilities were observed, and subsequent beam-based measurements combined with impedance modeling identified the HOMs trapped in small cavity-like structures of the vacuum gate valves as the most likely driving source [3].

To address this, we have performed macroparticle tracking simulations to study the longitudinal HOM-driven instabilities in the HALF storage ring. Under the condition of bunch lengthening provided by the HC, the dependence of the instability growth rate on HOM parameters, specifically resonant frequency and shunt impedance is thoroughly examined. The primary goal is to obtain quantitative longitudinal impedance thresholds that can directly guide the design and impedance optimization of vacuum components, ensuring stable high-current operation in HALF.

* Work supported by the National Natural Science Foundation of China (No. 12475158, No. 12341501 and No. 12375324).
† htlong@ustc.edu.cn

SIMULATION STUDIES

The main parameters of the HALF storage ring relevant to longitudinal dynamics are summarized in Table 1. Although we plan to adopt uniformly distributed gaps with 90% fill ratio to suppress ion instabilities, for simplicity we consider only the uniform fill case in this study. The short-range wakefield induced bunch profile distortion is also neglected.

Table 1: Main Parameters of the HALF Storage Ring

Parameter	Symbol	s
Circumference	C	479.86 m
Beam energy	E_0	2.2 GeV
Beam current	I_0	350 mA
Harmonic number	h	800
MC voltage	$V_{\rm rf}$	1.2 MV
Energy loss per turn	U_0	380 keV
Momentum compaction	α_p	9.4×10^{-5}
Natural rms bunch length	σ_{t0}	7.16 ps
Natural energy spread	$\sigma_{\delta 0}$	7.44×10^{-4}
HC R/Q	R/Q	40.5 Ω
HC quality factor	$Q_{\rm HC}$	2×10^8
Longitudinal damping time	τ_z	14 ms

Our simulations are carried out using the STABLE code [4], a GPU-accelerated macroparticle tracking framework originally developed for longitudinal beam dynamics studies. For a Gaussian bunch distribution and a uniform fill pattern, the growth rate of the longitudinal coupled-bunch instability driven by a narrow-band HOM can be expressed as [5]

$$\alpha_\ell = \frac{eI_0\alpha_p}{4\pi E_0 \nu_s} \sum_{p=-\infty}^{\infty} \omega_{p,\ell}\, \mathrm{Re}\, Z_\parallel(\omega_{p,\ell})\, e^{-(\omega_{p,\ell}\sigma_t)^2} \quad (1)$$

where $\omega_{p,\ell} = (ph + \ell + \nu_s)\omega_0$, ℓ is the coupled-bunch mode index, ν_s the synchrotron tune, ω_0 the angular revolution frequency, and σ_t the rms bunch length. For a single resonator impedance of the form

$$Z_\parallel(\omega) = \frac{R_s}{1 + iQ\left(\frac{\omega_r}{\omega} - \frac{\omega}{\omega_r}\right)}, \quad (2)$$

the sum is typically dominated by a single revolution harmonic p_0 when the HOM bandwidth is narrow compared to the revolution frequency. The maximum growth rate then occurs near resonance, where $\omega_r \approx (p_0 h + \ell + \nu_s)\omega_0$.

The passive HC controls the bunch length by adjusting its detuning frequency $\Delta f_{r,\rm HC}$. Figure 1 shows the longitudinal

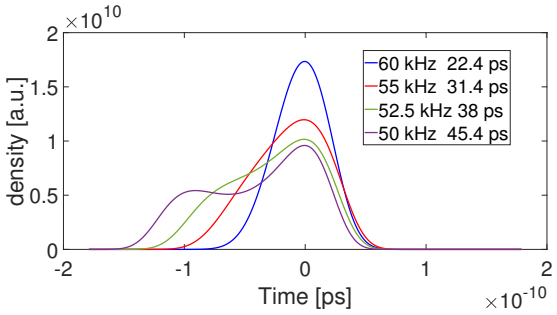

Figure 1: Longitudinal bunch profiles for different harmonic cavity detuning frequencies.

bunch profiles and the corresponding rms bunch lengths for different harmonic cavity detuning frequencies obtained by the semi-analytical method [6]. For moderate bunch lengthening up to a factor of about 3, the bunch profile in HALF remains approximately Gaussian, and the Eq. (1) still provides a reasonable estimate. At larger lengthening factors, the profile deviates from a Gaussian distribution, and the optimum lengthening condition does not correspond to a flat potential. A more general theoretical framework for arbitrary RF potentials has been developed by Lindberg [7], and we have attempted to implement its numerical solution. Unfortunately, our current implementation is not yet sufficiently robust for systematic parameter scans. Therefore, in this work we rely exclusively on macroparticle tracking simulations to evaluate the instability behavior. In the tracking simulations, each bunch is represented by 50,000 macroparticles, and 100 bunches are tracked to accelerate the computation. This number of bunches does not correspond to the actual fill pattern of HALF but is chosen solely for computational efficiency and it usually does not affect the accuracy of the instability growth rate evaluation. Radiation damping and quantum excitation effects are included in the simulations.

In the following, we present simulation results for different HOM parameters, starting with the gate valve case around 7.75 GHz and then extending to other frequency ranges.

The quality factor of the gate valve HOM is set to 40 000, so that the coupled-bunch instability is dominated by a single mode, which simplifies the instability analysis. In the simulations, the HOM resonant frequency is set to $12410 f_0$, where $f_0 \approx 625$ kHz is the revolution frequency. The factor 12 400 is chosen to bring the resonant frequency close to the expected gate valve HOM frequency of 7.75 GHz, while the remaining 10 corresponds to the coupled-bunch mode number ℓ that is most strongly excited.

To determine the instability threshold with $\Delta f_{r,\mathrm{HC}} = 55$ kHz, we scan the shunt impedance R_s of the gate valve HOM in steps of 2 kΩ and track the beam for a sufficiently large number of turns. Figure 2(a) shows the logarithm of the centroid energy deviation as a function of turn number for different values of R_s. The instability threshold can be directly identified: the beam remains stable up to 10 kΩ, while clear exponential growth of the centroid oscillation is observed for $R_s \geq 12$ kΩ, indicating that the threshold lies between 10 and 12 kΩ.

For the cases above threshold ($R_s \geq 12$ kΩ), the instability growth rate can be extracted by fitting the linear region of the logarithmic amplitude. The growth rates obtained directly from the simulations are shown as blue squares in Fig. 2(b), and the linear fit to these points is shown as the blue solid line. The corresponding values corrected by adding the radiation damping rate are shown as the red dashed line. The fact that the red curve does not cross zero at $R_s = 0$ indicates the presence of additional Landau damping associated with the bunch lengthening provided by the harmonic cavity.

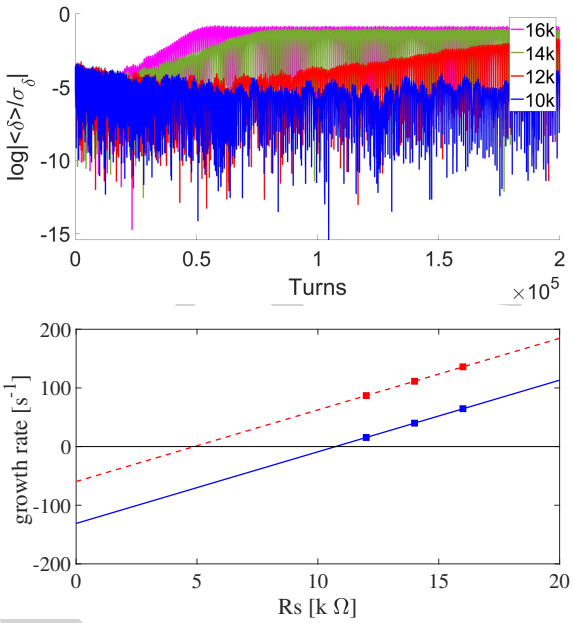

Figure 2: (a) Evolution of the centroid energy deviation for different R_s values (b) Fitted growth rates versus R_s at 7.75 GHz and $\Delta f_{r,\mathrm{HC}} = 55$ kHz.

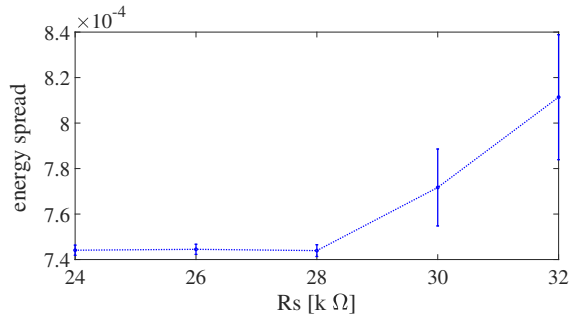

Figure 3: Energy spread versus Rs at 7.75GHz and $\Delta f_{r,\mathrm{HC}} = 52.5$ kHz.

When the detuning frequency of the harmonic cavity is set to 52.5 kHz, we perform the same scan of R_s in steps of 2 kΩ. In this case, no clear centroid oscillation similar to that shown in Fig.2(a) is observed. Instead, for R_s exceeding 30 kΩ, the energy spread of the bunches begins to increase, resembling the behavior of single-bunch microwave instability. Nevertheless, the relative phases of the

bunch centroid motion still follow the pattern characteristic of coupled-bunch instability modes. Figure 3 shows the energy spread as a function of R_s, where the error bars represent the rms amplitude of the energy spread oscillation. The threshold is found to lie between 28 and 30 kΩ, and a more precise determination can be obtained by reducing the step size of the R_s scan.

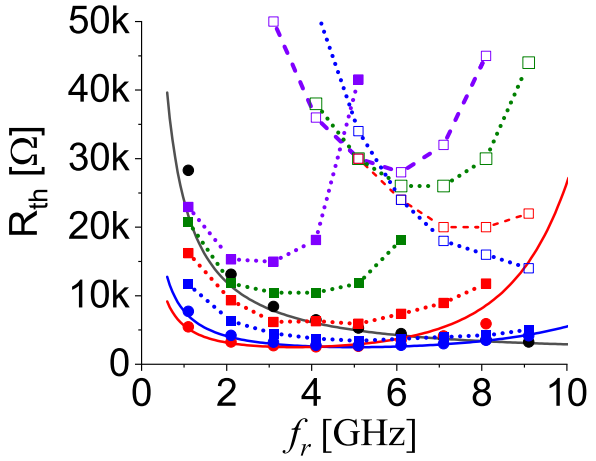

Figure 4: HOM shunt impedance threshold versus frequency for different bunch distributions.

The above analysis is extended to different HOM frequencies, and the results are summarized in Fig. 4. Different colors represent different bunch lengths or harmonic cavity detuning frequencies, following the same color scheme as in Fig. 1. The black color corresponds to the case without harmonic cavity, i.e., the natural bunch length. The solid line corresponds to the analytical prediction of Eq. (1) for a Gaussian bunch distribution. The circles are the simulation results under the Gaussian-bunch condition, obtained with a linear RF voltage whose slope is matched to the corresponding bunch length, which agree well with the analytical formula. The colored dashed lines represent the double-RF system with different harmonic cavity detuning frequencies and these lines simply connect the simulation data points. The solid square markers indicate the threshold at which clear centroid oscillations appear, determined using the same method as in Fig. 2. The open square markers indicate the threshold at which energy spread growth is observed, similar to the behavior shown in Fig. 3.

At high frequencies, the energy-spread-growth type of instability occurs first, i.e., at a lower shunt impedance than the centroid-oscillation type. At low frequencies, however, the centroid-oscillation type appears first, and can be suppressed by a longitudinal bunch-by-bunch feedback system, for example with a damping time of 1 ms, but after such suppression the energy-spread-growth type instability eventually emerges at higher impedance.

SUMMARY AND DISCUSSION

Longitudinal coupled-bunch instabilities driven by HOMs in the HALF storage ring have been studied via macroparticle tracking simulations, focusing on the gate valve HOM around 7.75 GHz and extending to a broader frequency range under different bunch lengthening conditions.

Two instability types are observed. The first, dominant at lower frequencies, features exponential centroid oscillation; its growth rate scales linearly with shunt impedance and can be suppressed by a longitudinal feedback system. The second, dominant at higher frequencies and stronger bunch lengthening, appears as energy spread growth without significant centroid motion. The instability threshold as a function of HOM frequency and harmonic cavity detuning has been mapped, providing quantitative impedance limits for the design of HALF vacuum components, including the gate valves.

Future work will include the inclusion of short-range wakefields, non-uniform fill patterns, and further theoretical analysis for arbitrary bunch distributions.

REFERENCES

[1] Z. Bai *et al.*, "A Modified Hybrid 6BA Lattice for the HALF Storage Ring", in *Proc. IPAC'21*, Campinas, Brazil, May 2021, pp. 385–388. doi:10.18429/JACoW-IPAC2021-MOPAB112

[2] R. Nagaoka and K. L. F. Bane, "Collective effects in a diffraction-limited storage ring", *J. Synchrotron Radiat.*, vol. 21, pp. 937–960, 2014. doi:10.1107/S1600577514015215

[3] M. B. Alves and F. H. de Sa, "Beam-based characterization of longitudinal coupled-bunch instabilities at SIRIUS storage ring", in *Proc. IPAC'25*, Taipei, Taiwan, Jun. 2025, pp. 2218–2221. doi:10.18429/JACoW-IPAC2025-WEPM104

[4] T. He and Z. Bai, "Graphics-processing-unit-accelerated simulation for longitudinal beam dynamics of arbitrary bunch trains in electron storage rings", *Phys. Rev. Accel. Beams*, vol. 24, p. 104401, 2021. doi:10.1103/PhysRevAccelBeams.24.104401

[5] K. Y. Ng, *Physics of Intensity Dependent Beam Instabilities*, Singapore: World Scientific, 2006. doi:10.1142/5835

[6] T. He, W. Li, Z. Bai, and L. Wang, "Longitudinal equilibrium density distribution of arbitrary filled bunches in presence of a passive harmonic cavity and the short range wakefield", *Phys. Rev. Accel. Beams*, vol. 24, p. 044401, 2021. doi:10.1103/PhysRevAccelBeams.24.044401

[7] R. R. Lindberg, "Theory of coupled-bunch longitudinal instabilities in a storage ring for arbitrary rf potentials", *Phys. Rev. Accel. Beams*, vol. 21, p. 124402, 2018. doi:10.1103/PhysRevAccelBeams.21.124402